Resistor mesh model of a spherical head: Part 1: Applications to scalp potential interpolation

N. Chauveau[1] J. P. Morucci[1,2] X. Franceries[2] P. Celsis[1]
B. Rigaud[2,3]

[1]Institut National de la Santé et de la Recherche Médicale, Toulouse, France
[2]Paul Sabatier University, Toulouse, France
[3]Jean-François Champollion University Center, Castres, France

Abstract—*A resistor mesh model (RMM) has been implemented to describe the electrical properties of the head and the configuration of the intracerebral current sources by simulation of forward and inverse problems in electroencephalogram/event related potential (EEG/ERP) studies. For this study, the RMM representing the three basic tissues of the human head (brain, skull and scalp) was superimposed on a spherical volume mimicking the head volume: it included 43 102 resistances and 14 123 nodes. The validation was performed with reference to the analytical model by consideration of a set of four dipoles close to the cortex. Using the RMM and the chosen dipoles, four distinct families of interpolation technique (nearest neighbour, polynomial, splines and lead fields) were tested and compared so that the scalp potentials could be recovered from the electrode potentials. The 3D spline interpolation and the inverse forward technique (IFT) gave the best results. The IFT is very easy to use when the lead-field matrix between scalp electrodes and cortex nodes has been calculated. By simple application of the Moore–Penrose pseudo inverse matrix to the electrode cap potentials, a set of current sources on the cortex is obtained. Then, the forward problem using these cortex sources renders all the scalp potentials.*

Keywords—*EEG/ERP, Modelling, Interpolation, Resistor*

Med. Biol. Eng. Comput., 2005, **43**, 694–702

1 Introduction

NEW INSIGHTS into the normal functions and pathologies of the human brain have been provided by the emergence, in the last two decades, of novel non-invasive neuro-imaging techniques. Functional magnetic resonance imaging (fMRI) and positron emission tomography can dynamically scan the entire brain with high sensitivity, allowing for mapping of haemodynamic measurements as well as of neurotransmitter and receptor uptake and regulation. FMRI provides haemodynamic measurements with excellent spatial resolution (in the order of millimetres) but is limited in its temporal resolution by the latency of the haemodynamic response (in the order of seconds), curtailing the ability of this technique to follow the high-frequency components of the temporal evolution of the neural activity underlying brain functions. Conversely, electro-encephalography (EEG) provides excellent temporal resolution (in the order of milliseconds), but uncertain spatial localisation of brain generators. A combination of information from electrophysiological and haemodynamic imaging modalities provides both high spatial and high temporal resolution.

Correspondence should be addressed to Dr Nicolas Chauveau; email: nicolas.chauveau@toulouse.inserm.fr

Paper received 6 July 2005 and in final form 17 October 2005
MBEC online number: 20054066

As EEG/event-related potentials (ERPs) are recorded from a limited number of electrodes on the scalp, interpolation is necessary using a finite difference method (FDM), finite element method (FEM) or boundary element method (BEM), so that the neuronal activity in the brain can be located. Accurate 3D analysis of EEG/ERP data through electric head models requires accurate representation of both the head geometry and head tissue conductivities.

The microscopic electrical properties that describe the interaction of an electromagnetic wave with matter are the complex conductivity σ^* and the complex permittivity ε^*. These parameters are tensors that become frequency dependent scalars, if it is assumed that the properties of the tissues are isotropic, linear and independent of time. Therefore the interaction between the electric current and the biological media can be modelled by equivalent electric circuits mimicking healthy and pathological tissues, and these models have allowed significant developments in the knowledge concerning living tissues.

Considering that the source frequency range is low in the brain ($\sim$10–50 Hz), the mathematical description of the potential and current flow fields can be done as if steady-state conditions existed at any instant, and, in practice, only real conductivities have to be taken into account.

A brain model using resistor networks has been implemented to describe the electrical properties of the head and the configuration of the intracerebral current sources. Interest in

modelling the brain by resistors and solution of the Poisson and Laplace equations has been outlined (FRANCERIES *et al.*, 2003) by showing the results of this approach in comparison with the analytical model.

As an analytical solution can be computed for a spherical geometry only, we also implemented a spherical model in the present work to permit validation. The study focused on interpolation techniques for Part 1 and cortical imaging using information from electrophysiological and haemodynamic imaging modalities for Part 2. Application to the real head will be developed in a future paper, using the most effective interpolation techniques and the best algorithms of cortical imaging obtained in this study.

2 Resistor mesh model

The chosen three-sphere head model represents the three basic tissues of the human head: brain, skull and scalp. Although the values of skull and scalp conductivity are likely to vary over a range (OOSTENDORP *et al.*, 2000), a ratio of 80 between both is used in this study, a value that has been commonly used by the authors (RUSH and DRISCOLL, 1969). Scalp and brain conductivity was set to 0.33 $S.m^{-1}$, and skull conductivity was set to 4.2 $mS.m^{-1}$ (GEDDES and BAKER, 1967). The inner, middle and outer radii of the three concentric spheres are, respectively, 72, 79 and 85 mm (standard model). The brain sources are modelled by dipoles defined by six parameters: location (r, θ_{loc}, φ_{loc}), orientation (θ_{ori}, φ_{ori}) and the dipolar moment M, defined by $M = Id$, where I is the primary current source propagating between the two poles of the source, and d is the distance between poles. The analytical solution was programmed using Matlab with 1° resolution for the θ and φ angles. This program calculates the surface potentials for any dipole placed in the spherical head model, using spherical co-ordinates.

A new modelling approach based on a resistor mesh is proposed. The spherical resistor mesh model (RMM) was designed to reproduce the analytical three-sphere model described above, each resistor representing a volume element of given geometry and conductivity (FRANCERIES *et al.*, 2003; CHAUVEAU *et al.*, 2004). The RMM was built with resistors oriented in the radial (e_r), tangential theta (e_θ) and tangential phi (e_φ) directions. This amounted to sampling of the whole spherical volume at 10° angular increments, considering 23 concentric spheres, and resulted in 14 122 nodes. The electrode cap angles, using the international 10–20 system, were matched to fit with the existing nodes of the spherical RMM (to within 10°). Each layer is represented by 617 nodes for the full sphere and 325 for the superior half sphere.

It is then possible to calculate the potentials at nodes, given one or several dipoles, using the Newton–Raphson algorithm programmed using MATLAB. In this case, the admittance matrix $\boldsymbol{Y}$, which is a sparse square symmetric matrix, needs to be calculated. This algorithm calculates potential values at all nodes in the spherical volume, and calculation is stopped when the relative error reaches a threshold that can be set as low as 10^{-15}. Accurate results are obtained with a threshold of only 10^{-8} (CHAUVEAU *et al.*, 2004). This RMM, which is a hybrid method between the finite difference method (FDM) and the transmission-line-matrix method (TLMM), permits the potentials in all the spherical volume to be calculated with accurate results compared with those produced at the scalp surface by the analytical solution, whatever the source eccentricity (FRANCERIES *et al.*, 2003).

3 Validation of the RMM

Validation of the RMM was achieved by applying the same dipole moments in the RMM and in the analytical model for four dipoles: two radial (radial right, (RR) and radial left (RL) and two tangential (tangential right (TR) and tangential left (TL)), each in the upper hemisphere and close to the cortex, giving a potential distribution all over the scalp. The co-ordinates are gathered in Table 1.

In the analytical model, locations θ_0, φ_0 and orientations θ_v, φ_v of the sources were considered with a dipole moment of $M = 20$ nA.m. For the analytical and resistor mesh models to be compared, the location, orientation and moment of the current dipole must be the same in both models.

In the RMM, a current dipole is simulated as follows: an ideal electrical current source I is placed between the two nodes that have been chosen to reproduce the dipole orientation, the middle corresponding approximately to the position of the point dipole in the analytical model. The resistor present between these nodes acts as an equivalent 'current dipole volume' of length d. Therefore the simulation of the dipole moment is achieved according to the equation $M = J_s S d = I d$, where d is the length between the connecting nodes J_s denotes the current density, and S is the surface of the equivalent resistor volume, perpendicular to the current.

In Fig. 1, the positions of the dipolar sources are reported on three different layers corresponding to 70, 69 and 64 mm. This particular configuration will permit us, in Part 2, to test the sensitivity of different inverse techniques to sources situated on close, but different, layers. Dipole RR has 1 mm length between the positive and negative currents defining the dipole and can be considered as a quasi punctual dipole. Poles are at a distance of 5 mm for RL and 7.8 mm for TR and TL: they represent volume sources.

Table 1 Dipole specifications in analytical model and in RMM. In analytical model, dipole is defined by origin (θ_0 φ_0), orientation (θ_v φ_v), eccentricity ($ecc = r/R$) and dipolar moment $M = 20$ nA.m. In RMM, dipole is defined by polar position (R, θ and φ) and intensity of each current of dipole(+/−1), such as $M = I.d = 20$ nA.m. For dipoles RR and RL, distance is $d = (R+)-(R-)$, and, for TR and TL, $d = R \sin(40°)\ \pi\ 10/180 = 7.8$ mm

Analytical	θ_0, deg	φ_0, deg	θ_v, deg	φ_v, deg	r/R	ecc
Dipole RR	80°	300°	80°	300°	70/85	0.82
Dipole RL	80°	240°	80°	240°	69/85	0.81
Dipole TR	40°	50°	90°	140°	70/85	0.82
Dipole TL	40°	140°	90°	50°	69/85	0.81
RMM	$R-$, mm	R+, mm	θ deg	φ, deg	current, A	d, mm
Dipole RR	69	70	80°	300°	$+/-2 \times 10^{-5}$	1
Dipole RL	64	69	80°	240°	$+/-4 \times 10^{-6}$	5
Dipole TR	70	70	40°	40°/50°	$+/-2.5 \times 10^{-6}$	7.8
Dipole TL	69	69	40°	140°/130°	$+/-2.5 \times 10^{-6}$	7.8

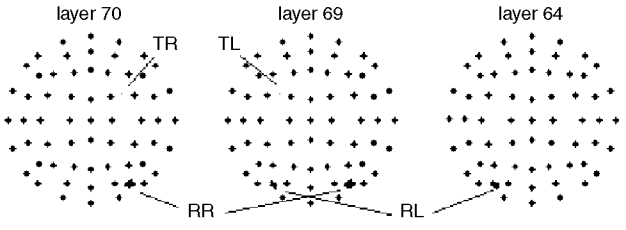

Fig. 1 *Position of current sources on three surface layers at 70, 69 and 74 mm. (◆) Projections of 61 electrodes on different corresponding layers*

Thanks to the RMM, the forward solution permits us to obtain the potentials at all nodes everywhere in the volume, in particular at the cortex surface. The reference point in the mesh model differs from the one in the analytical model. To make comparison possible, the potentials issued from both models were recalculated thanks to a method widely used in EEG and known as the 'common reference' method. It consists in subtracting the mean potential value from each voltage, which amounts to centring each data set around a mean value equal to zero. The potential distributions on the scalp for the two models are shown in Figs 2 and 3. Fig. 2 shows the scalp potentials and scalp current density (SCD) (PERRIN *et al.*, 1987*b*) on the isosurface obtained with the analytical solution. Fig. 3 displays the scalp and cortex potentials obtained with the forward solution applied to the resistor mesh model.

Several remarks can be made:

- the small differences between the scalp maps are due to the difficulty of ensuring exactly the same origin and orientation in both models for the dipoles: the dipole is punctual in the analytical model and placed between two nodes in the RMM
- the maxima of scalp potentials do not match any electrode, which is often the case for *in vivo* studies
- the SCD from the analytical solution and cortex potentials from the resistor model exhibit negative and positive areas at comparable locations, confirming the assertion that the SCD gives a good position estimation of the cortex activity
- the factor of 50 observed between the scalp and cortex potential scales is due to the drop of potential between cortex and scalp.

Data comparison was carried out, and errors were evaluated with reference to the analytical solution, using formulations of the magnification factor (MAG) and of the relative difference measure (RDM) that derive from MEIJS *et al.* (1989).

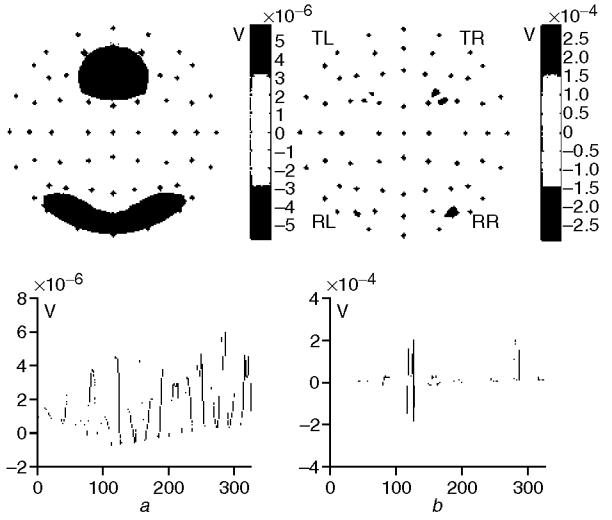

Fig. 3 *(a) Scalp potentials and (b) cortex potentials obtained with RMM. Upper drawings represent maps, and lower ones represent potentials as function of layer node indices (1–325)*

If the fitting were perfect, the MAG would be equal to one and the RDM would be equal to zero. Results of the comparison of both models are summarised in Fig. 4, which presents the MAG and RDM computed with all 325 scalp surface nodes on the hemisphere and for the 61 electrodes of a international 10-20 cap.

For scalp potential distributions, the MAG ranges from 0.98 to 1.01 for the four dipoles, and the RDM ranges from 0.02 to 0.04 for the radial dipoles and from 0.12 to 0.15 for the tangential ones. The relatively poor RDM for tangential dipoles can be explained by their length, resulting from the resolution of 10° in the θ angle. For the four-dipole configuration, the magnitudes of the potentials are similar to those calculated on the analytical model, although slightly overestimated (1% at maximum). The spatial distributions fit well, with a correlation coefficient better than 0.98. Thus the present validation of the mesh model complements the previous study (FRANCERIES *et al.*, 2003), which compared the MAG and RDM obtained with the RMM with data from the literature (THEVENET *et al.*, 1991; YVERT *et al.*, 1995; MATTOUT, 2002), computed on FDM, BEM and FEM models for tangential dipoles simulated at various eccentricities on the x-axis and processed by the common reference method. In every case, the reference model was a three-sphere model.

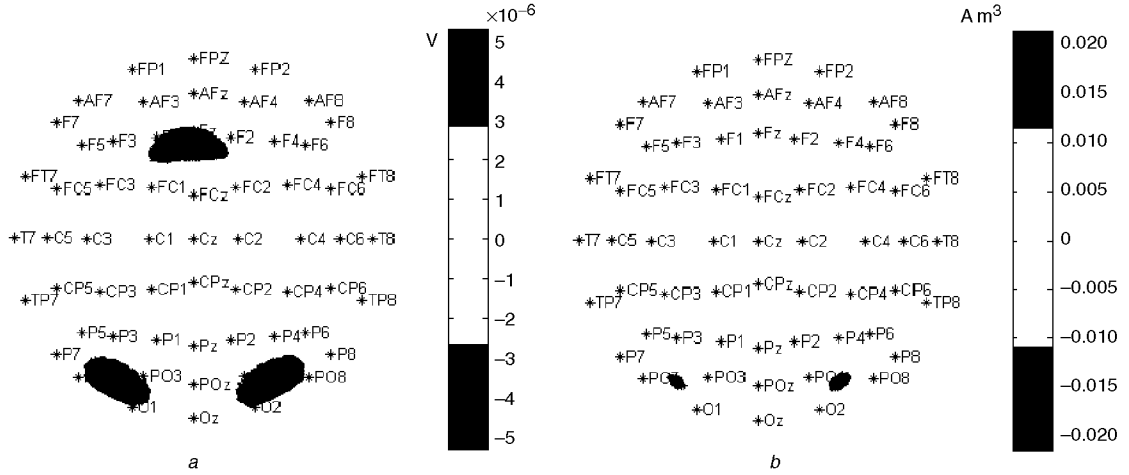

Fig. 2 *(a) Scalp potentials and (b) scalp current density (SCD) obtained with analytical solution. Each electrode position has been fitted to closer surface node*

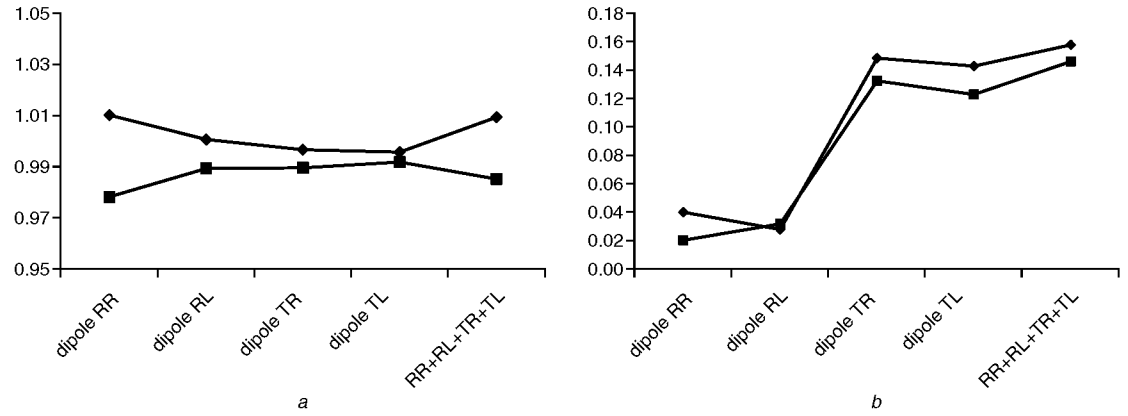

Fig. 4 *(a) MAG and (b) RDM for RMM with analytical solution as reference. Dipole RR-radial right; RL-radial left, TR-tangential right; TL-tangential left. Last case is four dipoles together. (a) (–◆–) MAG 1/2 sphere, 325 points; (–■–) MAG cap, 61 electrodes. (b) (–◆–) RDM 1/2 sphere, 325 points; (–■–) RDM cap, 61 electrodes*

4 Interpolation methods

4.1 *Introduction*

To allow a valuable estimation of the cortical potentials and owing to the low number of electrodes used for data acquisition (32, 64, ...) in event-related potential (ERP) recording, interpolation is necessary to estimate the signal everywhere between the electrodes. The spherical methods consider the 3D head scalp as a hemispherical surface, the hemisphere being a crude anatomical approximation of the human head. The axes Ox, Oy, Oz are affected at the following co-ordinates: centre of the sphere O (0, 0, 0), central electrode Cz (0, 0, 1), nasion (0, 1, 0) and inion (0, −1, 0). The map is obtained thanks to interpolated potentials on the hemisphere.

Many different and sometimes contradictory results of interpolation studies have already been reported. In clinical EEG, interpolation from 31 electrodes gives good results when the alpha rhythm is studied. According to KOLES *et al.* (1989), '*Bilinear and bicubic splines produce precise estimates of scalp potential in the delta, theta and alpha frequency band but poor estimates in the beta band*', and, according to SOUFFLET *et al.* (1991), '*Barycentric, polynomial, spline give better spatial resolution than with standard planar mapping*'. Some authors are more pessimistic about interpolation; for instance, BIGGINS *et al.* (1991) argue that '*Major artefact is introduced by using spherical spline procedure*', and SOONG *et al.* (1993) recommend that '*Interpolation should not be used with electrode densities of the order provided by the international 10–20 system neither to increase the spatial resolution nor in more sophisticated analysis techniques as SCD*'.

The general concepts leading to the elaboration of interpolation methods belong to four distinct families (nearest neighbour, polynomial, splines and lead fields), and all these methods have been compared using as reference the 325 potential values obtained on the RMM (Fig. 3) from the 61 potential values at the electrode locations.

4.2 *Methods*

4.2.1 *Nearest neighbour methods: 3D barycentric interpolation*

The nearest-neighbour (NN) technique is a simple method of interpolating the data. The potential value interpolated at a given point M on the scalp is the weighted sum of the potential values attributed to each of the electrodes. The weight attributed to each electrode is a function of the Euclidian distance between the electrode and the point M. The barycentric interpolation used here is the local one and only attributes a weight to the electrodes closest to the point M. The estimated value for point M on the scalp with the mth order of the interpolation and for the k nearest electrodes is given by

$$V(M) = \frac{\sum_{i=1}^{k} V(e_i) d_i^{1-m}}{\sum_{i=1}^{k} d_i^{1-m}}$$

where $V(e_i)$ is the potential at the ith electrode located at $\boldsymbol{E}_i = (x_i, y_i, z_i)$, and d_i is the distance from the point M to this electrode (PERRIN *et al.*, 1987).

Spherical barycentric interpolation: The Euclidian distance between the electrode and the point M used for the 3D barycentric interpolation is replaced by the corresponding curvilinear distance on the sphere.

Laplacian minimisation method (surface Laplacian): As no sources are located at the scalp surface, the Laplace equation can be applied to the scalp. Interpolation is accomplished by minimisation of the Laplacian of the potential at all head surface nodes (i.e. 61 with known potentials and 264 to be interpolated), thereby constraining the interpolated potentials to have a smooth spatial second derivative over the half-head surface. Oostendorp and van Oosterom introduced this method for body surface potential maps (OOSTENDORP and VAN OOSTEROM, 1996), and it was been later presented by HOEKEMA *et al.* as a transformation method of potential maps on the body for different electrode configurations (HOEKEMA *et al.*, 1995).

4.2.2 *3D polynomial method*

3D polynomial interpolation: In the 3D polynomial interpolation, every interpolated value can be computed by means of only one polynomial of three variables. ASHIDA *et al.* proposed the use of polynomial interpolators (ASHIDA *et al.*, 1984), the maximum order of which depends on the number of electrodes and that minimises the sum of square differences between the measured values and the interpolated ones. The Ashida formulas for 3D representation have been transposed by SOUFFLET *et al.* (1991). Thus, at the position $M(x, y, z)$, the estimated value $V(x, y, z)$ is expressed by a 3D isotropic mth-order symmetric polynomial, as follows:

$$f(s, y, z) = \sum_{L=0}^{m} \sum_{i+j+k=L} a_{ijk} x^i y^j z^k$$

where (a_{ijk}) are the coefficients of the polynomial. The interpolation has been calculated for m varying from 2 to 5, to satisfy

the relationship

$$\sum_{i=1}^{m+1} i(m-i+2) \leq Ns$$

where $Ns = 61$ is the number of electrodes.

Spherical polynomial interpolation: On a sphere, the position of some point $M(x, y, z)$ can be defined thanks to only two angular co-ordinates θ_x and θ_y. Thus, the polynomial interpolation method proposed by ASHIDA *et al.* in 2D can be implemented using these two angular co-ordinates. At the position $M(\theta_x, \theta_y)$, the estimated value $V(\theta_x, \theta_y)$ of the potential can be expressed by a 2D isotropic mth-order symmetric polynomial as follows

$$f(\theta x, \theta y) = \sum_{k=0}^{m} \sum_{i=0}^{k} a_{k-i,i} \theta_x^{k-i} \cdot \theta_y^i$$

The interpolation has been calculated for m varying from 2 to 10 to satisfy the relationships

$$(m+1)(m+2) \leq 2Ns$$

where $Ns = 61$ electrodes.

4.2.3 *Spline methods*

Two spline interpolation schemes are used commonly in EEG/ERP research:

(i) The spherical splines (PERRIN *et al.*, 1987a; 1989) assume spherical head geometry.
(ii) The three-dimensional splines were introduced by PERRIN *et al.* (1987*a*), in the context of two-dimensional polar projections of EEG data, and were extended to full three-dimensional geometry by LAW *et al.* (1993) and SRINIVASAN *et al.* (1996).

Spherical spline technique: Spherical splines were first proposed as an interpolator for sampled data on a sphere by WAHBA (1981; 1982) for a meteorological application. If the bending energy is written in its integral form, it can be shown, using the calculus of variations, that the deflection (or potential) at point p on the surface of the sphere can be written as

$$v(p) = \sum_{i=1}^{N_s} c_i q_m(p - p_i) + d$$

where N_s is the number of electrodes, and

$$q_m(p, p_i) = \frac{1}{4\pi} \sum_{\mu=1}^{\infty} \frac{2\mu+1}{\mu_m(\mu+1)_m} P_\mu(\cos(p, p_i))$$

where $P\mu$ is the μth degree Legendre polynomial, and (p, p_i) is the angle between the point p and the p_i electrode location on the surface of the sphere. The coefficient vector c and the scalar d have to be determined. The performance of this interpolator has been evaluated for $m = 2$–6, and, as this interpolator requires the calculation of an infinite sum, the choice has to be made to determine a reasonable point of truncation at $m = 6$, which gives the same result as $m = 5$.

3D spline interpolation: The 3D surface spline method was first introduced as an interpolation method for use in aircraft design by HARDER and DESMARAIS (1972), extended by DUCHON (1976) on the 2D flexion of thin plates and later modified for use in EEG mapping for freely distributed electrodes (SOUFFLET *et al.*, 1991). Duchon has shown that the theory of surface splines can be extended to 3D interpolation (DUCHON, 1976), and the D_m spline functions (m order of the spline) have m continuous derivatives. This interpolation minimises the bending energy of an infinitely thin plate (i.e, the Laplacian of the Laplacian) and constrains the values to pass through the known scalp potentials. Let n be the total number of points of measurement, V_i be the measured value at the ith point of measurement E_i (x_i, y_i, z_i), and m be an integer >2. The 3D V_m spline function is defined as follows

$$V_m(x, y, z) = \left[\sum_{i=1}^{n} l_i \cdot N_{m-1}(x - x_i, y - y_i, z - z_i)\right] + P_{m-1}(x, y, z)$$

where P_{m-1} is a 3D polynomial of order $m - 1$

$$P(x, y, z) = \sum_{L=0}^{m-1} \sum_{i+j+k=L} a_{ijk} \cdot x_i \cdot y_j \cdot z_k$$

and

$$N_{m-1} = [(x - x_i)^2 + (y - y_i)^2 + (z - z_i)^2]^{m-1} \log[(x - x_i)^2 + (y - y_i)^2 + (z - z_i)^2 + w^2]$$

The mathematical formulation of the surface spline consists of two terms, a basis function N_{m-1} and P_{m-1} a polynomial. The 3D polynomial of order $m-1$ is known as the osculating function, which constrains the smoothness of the interpolation of the resulting surface distribution.

Several expressions of the basis function N_{m-1}have been proposed in the literature

$$N_{m-1} = [(x - x_i)^2 + (y - y_i)^2 + (z - z_i)^2]^{m-1}$$

(HARDY, 1971)

$$N_{m-1} = [(x - x_i)^2 + (y - y_i)^2 + (z - z_i)^2]^{(2m-3/2)}$$

(DUCHON, 1976)

$$N_{m-1} = [(x - x_i)^2 + (y - y_i)^2 + (z - z_i)]^{m-1} \log[(x - x_i)^2 + (y - y_i)^2 + (z - z_i)^2]$$

(SOUFFLET *et al.*, 1991; SOONG *et al.*, 1993).

$$N_{m-1} = [(x - x_i)^2 + (y - y_i)^2 + (z - z_i)^2]^{m-1} \log[(x - x_i)^2 + (y - y_i)^2 + (z - z_i)^2 + w^2]$$

by PERRIN *et al.*, (1987*a*).

The inclusion of w^2 is supposed to take into account the distributed potentials under the electrodes instead of punctual information. Two parameters have to be adjusted for applications to EEG. They are the order of the spline m and w, a constant that accounts for the finite size of the recording electrode. The interpolation is more flexible, but the matrix inversion becomes numerically unstable with increasing orders. Because of the function N_{m-1}, the quality of the interpolation depends strongly on the order m. Good results are obtained

with m in the general range of 0.5–3.0 (PERRIN *et al.*, 1987; PIDOUX and POIROT, 1990; LAW, 1991) and $w = 1.0$ cm: roughly the size of EEG electrodes.

Among a large variety of spline functions for use with scattered data (potential values at the electrodes), splines based on multiquadratic functions provide the most 'visually pleasing' results, without loss of accuracy and with robustness and ease of implementation (HARDY, 1971; NIELSON *et al.*, 1991).

The particular three-dimensional spline discussed here has been independently developed and applied to EEG by several groups (PERRIN *et al.*, 1987*a*; PIDOUX and POIROT, 1990; LAW, 1991). Their results suggest that this 3D spline provides good accuracy and flexibility for imaging brain electrical activity.

4.2.4 *Inverse forward method using lead fields*

This method is based on the use of an inverse lead-field technique (see Appendix 2) to estimate the equivalent cortical sources at the origin of the electrode cap potentials. The lead-field matrix is constructed by successive application of a unit current at each surface electrode and calculation of the cortex potentials using a forward solution. Then, the reciprocity theorem permits us to state that this result is equivalent to injecting currents at the cortex surface and measuring the scalp potentials at the scalp electrodes. The lead-field matrix is then obtained, inverted and applied to scalp electrode potentials, giving an estimation of sources at the cortex. Then, a forward solution (using the Newton–Raphson algorithm) is calculated using those sources. As this calculation gives the potentials at all nodes, an interpolation of the scalp potentials is obtained.

5 Results

The eight different interpolation methods were evaluated using six evaluation tests described in Appendix 1: the magnification factor (MAG), the relative difference measure (RDM), the normalised residual variance (NRV), the prediction covariance (CV), the residual covariance (RCV) and the maximum squared residual error (MSRE).

From the results in Table 2, three main conclusions emerge:

(*a*) The best results for each family depend on the order of the interpolation.

(*b*) The 3D spline interpolation gives, as largely published, the best results.

(*c*) The introduction of the log, which adds a weighting factor taking into account the distance to the electrodes, does not play an essential role in our example.

In addition, all the interpolation techniques are characterised by the inability to localise the extrema elsewhere than at the electrodes.

The best results for RDM and MAG are observed for spherical spline interpolation, 3D spline interpolation without log and power $(2m - 3)/2$, or with $\log(d)$, and also with the inverse forward (IF) technique. As spherical splines cannot be used on a realistic head model, they will not be considered any further. The best results, obtained with 3D spline interpolation without log and with the IF technique, are shown in Fig. 5.

The effects due to the level of noise and to the number of electrodes were tested by the addition of 2% of the maximum electrode potential to the electrode values as a random noise, and by an increase to 107 of the number of electrodes. Only MAG and RDM are reported for this study complement. The results are presented in Table 3, using 3D spline interpolation (formulation without log).

The addition of 2% noise to a 61-electrode cap does not change the quality of interpolation. The best interpolation with the 107-electrode cap is obtained with $m = 2$ instead of 5, and the 2% noise level does not change the results, as already published (ASHIDA *et al.*, 1984).

6 Discussion

In this paper, a new modelling approach based on the RMM has been presented to calculate the potential distribution in a volume conductor of any geometry and conductivity. Despite attempts to reproduce the electrical properties of cell membranes by resistances and capacitances (VALENTINUZZI *et al.*, 1996), there is a lack of volume-based electrical models that take into account the precise geometry of the simulated volume and are able to reproduce the propagation of currents elicited by brain sources in the head. Our contribution consists in mimicking both the geometry and the electrical properties of the volume conductor by resistors arranged in a mesh.

The concept at the root of the proposed RMM is based on the assumption that the problem described by the microscopic electrostatic laws can be turned into the question of dealing with the macroscopic Ohm's laws by solving Kirchhoff's equations. This approach simplifies the dimension of the problem and offers an easy method of solving Poisson's

Table 2 Interpolation validation of scalp potentials in comparison with forward solution in RMM, for potential values collected with 61-electrode cap for four dipoles applied at same time. Best results are presented, with interpolation parameter m providing minimum RDM value. This parameter has been chosen because it guarantees good correspondence of potential profiles

Interpolation method		m	MAG	RDM	NRV	CV	RCV	MSRE
Barycentric	linear distance	3	0.8310	0.3061	0.0515	0.9756	−0.4562	2.7084
	spherical distance	3	0.8312	0.3061	0.0515	0.9756	−0.4561	2.7084
Laplacian minimisation $\Delta V = 0$			0.8859	0.2250	0.0280	0.9870	−0.4543	2.5250
3D polynomial interpolation	3D	4	0.9027	0.2804	0.0390	0.9809	−0.3569	2.7234
	Spherical	8	0.9135	0.2388	0.0290	0.9861	−0.3794	2.4650
Spherical spline		5	0.9262	0.1650	0.0149	0.9931	−0.3889	1.5819
3D spline interpolation	without log $(2m - 3)/2$	5	0.9272	0.1648	0.0148	0.9931	−0.3758	1.4981
	without log $(m - 1)$	5	0.9027	0.2804	0.0390	0.9809	−0.3569	2.7234
	with $\log(1 + d)$	4	0.9269	0.1644	0.0148	0.9932	−0.3942	1.5374
	with $\log(d)$	5	0.9306	0.1676	0.0152	0.9930	−0.4033	1.4449
Inverse forward			0.91842	0.1794	0.0175	0.6331	−0.3522	1.9322

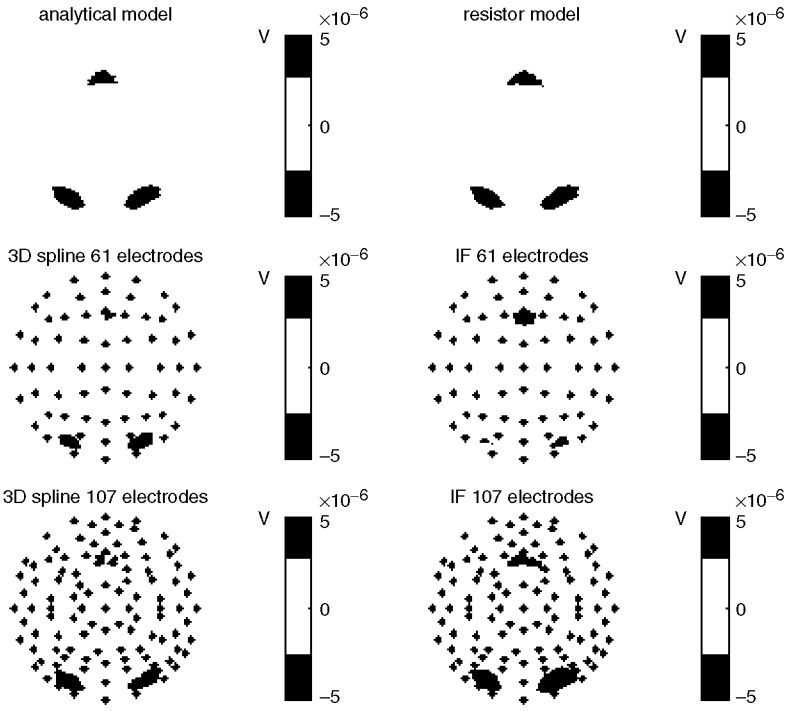

Fig. 5 *Comparison of scalp potentials between analytical model, RMM, and in RMM after interpolation using 3D spline or IFM from 61 and 107 electrode caps. IFM is obtained using first inverse lead fields and then forward method, starting from cortex currents previously estimated*

equation. Basically, a resistor allows only linear current propagation between both connecting nodes, which is a simplification of the current conduction in a volume. The spherical resistor mesh model, dedicated to simulation of the forward and inverse problems in EEG/ERP studies, has been described and validated with reference to the analytical model. This validation has been done for a set of four dipoles close to the cortex.

Most of the interpolation techniques published in the literature using spherical or Cartesian co-ordinates have been tested to recover the scalp potentials from the electrode potentials. The 3D spline interpolation and the inverse forward technique give the best results. Nevertheless, like all the other techniques, they are unable to recover a missed maximum potential, owing to the poor resolution of the electrode measurement cap. A higher number of electrodes, up to 128, increases the quality of the interpolation (JUNGHOFER *et al.*, 1997).

All these interpolation techniques have been compared, with a view to selecting the best ones to apply them to realistic heads modelled with RMM, in work that is in preparation.

Appendix 1

Evaluation methods of interpolation

The error in the interpolation was described using various measures, all based upon the difference between the predicted V_d and interpolated V_{int} potentials at each of the $N = 325$ nodes.

Magnification factor (MAG) and relative difference measure (RDM): MAG is an index of potential magnitude comparison, and RDM pertains to the fitting of potential spatial distribution between both models.

Provided V_{Ai} is the scalp potential at node i (given by the analytical solution on the three-sphere model) and V_{Si} is the corresponding simulated potential on the resistor mesh model, MAG and RDM are given by

$$MAG = \sqrt{\frac{\sum_{i=1}^{n} V_{Si}^2}{\sum_{i=1}^{n} V_{Ai}^2}}$$

$$RDM = \sqrt{\sum_{i=1}^{n} \left(\frac{V_{Si}}{\sqrt{\sum_{i=1}^{n} V_{Si}^2}} - \frac{V_{Ai}}{\sqrt{\sum_{i=1}^{n} V_{Ai}^2}} \right)^2}$$

where n is the number of nodes taken into account. Comparison of data from both models has been achieved by taking as many points as the number of scalp surface nodes in the considered mesh model. These equations show that MAG is an index of potential magnitude comparison, whereas RDM reflects the fitting quality of potential spatial distribution. RDM is also in direct connection to the linear correlation coefficient r: $RDM^2 = 2(1 - r)$.

Table 3 Effects of 2% noise and electrode number on interpolation. This is confirmation of low effect of adding 2% noise both for 61 and 107 electrodes

3D spline	m	MAG (no noise)	RDM (no noise)	MAG (2% noise)	RDM (2% noise)
61 electrodes	5	0.927	0.165	0.928	0.167
107 electrodes	2	0.987	0.154	0.989	0.157

If the fitting were perfect, MAG would be equal to one, and RDM would be equal to zero.

NRV,CV,RCV,MSRE: For node i with scalp potential $V(i)$, the residual potential $V_r(i)$ is defined as

$$V_r(i) = V_{int}(i) - V_d(i)$$

The variances of the predicted potentials V_d and of the residual potentials V_r are obtained from

$$\sigma_d^2 = \frac{1}{N}\sum_{i=1}^{i=N} V_d(i)^2 \quad \sigma_r^2 = \frac{1}{N}\sum_{i=1}^{i=N} V_r(i)^2$$

The covariance between the predicted and the interpolated potentials and that between the residual and measured potentials are obtained from

$$\sigma_{d.int}^2 = \frac{1}{N}\sum_{i=1}^{i=N} V_d(i).V_{int}(i) \quad \sigma_{r.d}^2 = \frac{1}{N}\sum_{i=1}^{i=N} V_d(i).V_r(i)$$

NRV: Based on the above formulas, the normalised residual variance (NRV) is obtained from

$$NRV = \frac{\sigma_r^2}{\sigma_d^2}$$

NRV is a measure of the inaccuracy of the interpolator, including both the error bias and its variance. NRV includes all the errors, systematic or random, in the interpolation technique and can be considered as the variance of that part of the potentials that is not accounted for by the interpolation technique. Hence, the value of NRV for a perfectly accurate interpolator would be zero.

CV: The precision of the interpolator is measured by the prediction covariance (CV) and is defined as

$$CV = \frac{\sigma_{d.int}^2}{\sigma_d \sigma_{int}}$$

CV is a measure of precision describing how closely the potentials predicted by the interpolation technique follow the potentials obtained by solution of the direct problem. As CV measures the deviation, due to random rather than systematic errors, of the interpolated potentials from the expected values, the value of CV for a perfectly precise interpolator would be 1.

RCV: As a measure of the correlation between the residual potentials and the direct potentials, the residual covariance (RCV) is given by

$$RCV = \frac{\sigma_{d.r}^2}{\sigma_d.\sigma_r}$$

The RCV measures whether the interpolation technique consistently over or underestimates the direct potentials and so it is considered a measure of bias. A negative value of RCV indicates a consistent underestimation, whereas a positive value indicates an overestimation. The value of RCV for an unbiased interpolator would be 0.

MSRE: Finally, an indication of the maximum error in the interpolation is given by the maximum squared residual error (MSRE), defined as

$$MSRE = \frac{\max[V_r^2(i)]}{\sigma_d^2}$$

As such, MSRE is a measure of tolerance, because it provides an indication of the range of the error between the interpolated potentials and the expected potentials. An interpolator with a high tolerance would yield a value for MSRE very near to 0.

Appendix 2

Lead fields

The lead-field (LF) approach is used in most imaging techniques. The mapping of intracerebral sources to scalp potentials can be represented by a linear operator ***LF***, the so-called *lead-field matrix*, which contains information about the geometry and conductivity of the model. The problem in brain source imaging is, given a set of potential recordings and knowing ***LF***, to determine the set of sources that gave rise to those potential values. This imposes the need to invert ***LF***, which is an ill-posed problem whose solution requires the application of a regularisation method.

The resistor mesh model makes the construction of this matrix easy by application of the reciprocity principle, which states that the voltage difference between two points A and B inside a volume conductor generated by a unit current applied between two surface electrodes C and D expresses how the same electrodes C and D record the same voltage difference caused by a unit current through points A and B. Therefore, rather than simulation of a source between each node pair of the cortex and computation of the potential at each electrode or node at the periphery, it is better to invert the process: simulating a current source between a pair of scalp electrodes and, for each pair, computing the resulting potentials of all the nodes in the mesh. As the mesh model is spherical with 0 reference potential at the centre of the sphere, all the current sources are perpendicular to the scalp surface: then, the lead-field matrix is built by injecting a unit current on each of the 61, or in some cases 107, electrode nodes and calculating potential values on each of the 325 cortex nodes. The notation used is $\boldsymbol{LF}_{325}^{n}$, with $n = 61$, 107 or 325.

References

ASHIDA, H., TATSUNO, J., OKAMOTO, J., and MARU, E. (1984): 'Field mapping of EEG by unbiased polynomial interpolation', *Comput. Biomed. Res.*, **17**, pp. 267–276

BIGGINS, C. A., FEIN, G., RAZ, J., and AMIR, A. (1991): 'Artifactually high coherences result from using spherical spline computation of scalp current density', *Electroencephalogr Clin Neurophysiol*, **79**, pp. 413–419

CHAUVEAU, N., FRANCERIES, X., DOYON, B., RIGAUD, B., MORUCCI, J. P., and CELSIS, P. (2004): 'Effects of skull thickness, anisotropy, and inhomogeneity on forward EEG/ERP computations using a spherical three-dimensional resistor mesh model', *Hum. Brain Mapp.*, **21**, pp. 86–97

DUCHON, J. (1976): 'Interpolation des fonctions de deux variables suivant le principe de la flexion des plaques minces', *RAIRO Anal Num*, **10**, pp. 5–12

FRANCERIES, X., DOYON, B., CHAUVEAU, N., RIGAUD, B., CELSIS, P., and MORUCCI, J. P. (2003): 'Solution of Poisson's equation in a volume conductor using resistor mesh models: application to event related potential imaging', *J. Appl. Phys.*, **93**, pp. 3578–3588

GEDDES, L. A., and BAKER, L. E. (1967): 'The specific resistance of biological material—a compendium of data for the biomedical engineer and physiologist', *Med. Biol. Eng.*, **5**, pp. 271–293

HARDER, R. L., and DESMARAIS, R. N. (1972): 'Interpolation using surface splines', *J Aircraft*, **9**, pp. 189–191

HARDY, R. L. (1971): 'Multiquadric equations of topography and other irregular surfaces', *J. Geophys. Res.*, **76**, pp. 1905–1915.

HOEKEMA, R., HUISKAMP, G. J., OOSTENDORP, T. F., UIJEN, G. J., and VAN Oosterom, A. (1995): 'Lead system transformation for pooling of body surface map data: a surface Laplacian approach', *J. Electrocardiol.*, **28**, pp. 344–345

JUNGHOFER, M., ELBERT, T., LEIDERER, P., BERG, P., and ROCKSTROH, B. (1997): 'Mapping EEG-potentials on the surface of the brain: a strategy for uncovering cortical sources', *Brain Topogr*, **9**, pp. 203–217

KOLES, Z. J., KASMIA, A., PARANJAPE, R. B., and MCLEAN, D. R. (1989): 'Computed radial-current topography of the brain: patterns associated with the normal and abnormal EEG', *Electroencephalogr. Clin. Neurophysiol.*, **72**, pp. 41–47

LAW, S. K. (1991): 'Spline generated surface Laplacian estimates for improving spatial resolution in electroencephalography'. *Ph D dissertation, Dept. Biomed Eng., Tulane Univ, New Orleans, LA* USA

LAW, S. K., NUNEZ, P. L., and WIJESINGHE, R. S. (1993): 'High-resolution EEG using spline generated surface Laplacians on spherical and ellipsoidal surfaces', *IEEE Trans. Biomed. Eng.*, **40**, 145–153.

MATTOUT, J. (2002): 'Approches statistiques multivariées pour la localisation de la localisation de l'activité cérébrale en magnétoencéphalographie et en imagerie par résonance magnétique fonctionnelle. Vers une fusion d'informations multimodales'. *Ph D dissertation, Univerté de Paris, VI., France*

MEIJS, J. W., WEIER, O. W., PETERS, M. J., and VAN OOSTEROM, A. (1989): 'On the numerical accuracy of the boundary element method', *IEEE. Trans. Biomed. Eng.*, **36**, pp. 1038–1049.

NIELSON, M., FOLEY, T. A., HAMANN, B., and LANE, D.. (1991): 'Visualizing and modeling scattering multivariate data', *IEEE Comput Graph Appl.*, **11**, pp. 47–55

OOSTENDORP, T. F., and VAN OOSTEROM, A. (1996): 'The surface Laplacian of the potential: theory and application', *IEEE. Trans. Biomed. Eng.*, **43**, pp. 394–405

OOSTENDORP, T. F., DELBEKE, J., and STEGEMAN, D. F. (2000): 'The conductivity of the human skull: results of *in vivo* and *in vitro* measurements', *IEEE Trans. Biomed. Eng.*, **47**, pp. 1487–1492

PERRIN, F., PERNIER, J., BERTRAND, O., GIARD, M. H., and ECHALLIER, J. F. (1987*a*): 'Mapping of scalp potentials by surface spline interpolation', *Electroencephalogr. Clin. Neurophysiol.*, **66**, pp. 75–81

PERRIN, F., BERTRAND, O., and PERNIER, J. (1987*b*): 'Scalp current density mapping: value and estimation from potential data', *IEEE Trans. Biomed. Eng.*, **34**, pp. 283–288

PERRIN, F., PERNIER, J., BERTRAND, O., and ECHALLIER, J. F. (1989): 'Spherical splines for scalp potential and current density mapping', *Electroencephalogr. Clin. Neurophysiol.*, **72**, pp. 184–187

PIDOUX, B., and POIROT, F. (1990): 'Tridimensional cartography of potentials recorded on the human scalp: I. Interpolation with tridimensional functions', *C. R. Acad. Sci. III*, **311**, pp. 1–6

RUSH, S., and DRISCOLL, D. A. (1969): 'EEG electrode sensitivity—an application of reciprocity', *IEEE. Trans. Biomed. Eng.*, **16**, pp. 15–22

SOONG, A. C., LIND, J. C., SHAW, G. R., and KOLES, Z. J. (1993): 'Systematic comparisons of interpolation techniques in topographic brain mapping', *Electroencephalogr. Clin. Neurophysiol.*, **87**, pp. 185–195

SOUFFLET, L., TOUSSAINT, M., LUTHRINGER, R., GRESSER, J., MINOT, R., and MACHER, J. P. (1991): 'A statistical evaluation of the main interpolation methods applied to 3-dimensional EEG mapping', *Electroencephalogr. Clin. Neurophysiol.*, **79**, pp. 393–402

SRINIVASAN, R., NUNEZ, P. L., TUCKER, D. M., SILBERSTEIN, R. B., and CADUSCH, P. J. (1996): 'Spatial sampling and filtering of EEG with spline laplacians to estimate cortical potentials', *Brain Topogr.*, **8**, pp. 355–366

THEVENET, M., BERTRAND, O., PERRIN, F., DUMONT, T., and PERNIER, J. (1991): 'The finite element method for a realistic head model of electrical brain activities: preliminary results', *Clin. Phys. Physiol. Meas.*, **12**, pp. 89–94

VALENTINUZZI, M. E., MORUCCI, J. P., and FELICE, C. J. (1996): 'Bioelectrical impedance techniques in medicine', *Crit. Rev. Biomed. Eng.*, **24**, pp. 353–466

WAHBA, G. (1981): 'Spline interpolation and smoothing on the sphere', *SIAM J. Sci. Stat. Comp*, pp. 5–16

WAHBA, G. (1982): 'Erratum: Spline interpolation and smoothing on the sphere', *SIAM J. Sci. Stat. Comp.*, pp. 385–386

YVERT, B., BERTRAND, O., ECHALLIER, J. F., and PERNIER, J. (1995): 'Improved forward EEG calculations using local mesh refinement of realistic head geometries', *Electroencephalogr. Clin. Neurophysiol.*, **95**, pp. 381–392

Author's biography

Nicolas Chauveau was born in 1954. He received the M.Sc. degree and the Ph.D degree in Biomedical Engineering from the University of Toulouse III, Toulouse, France, in 1977 and 1990 respectively. He works for the National Institute for Health and Medical Research (Inserm) As a research engineer. Automation of Extra-Corporeal Circulation has been his main interest for many years. Then, he has been working for 5 years in the field of Bioelectrical Impedance. In 2000, he joins U455 research unit, where he is mainly involved in realistic head models and inverse problems applied to EEG/ERP.